Simulation Methods of a Normal-Mode Helical Antenna in a Human Body Condition

Dang Tien Dung, Nguyen Quoc Dinh
Le Quy Don Technical University
Hanoi, Vietnam
Email: dangtiendung@tcu.edu.vn
dinhnq@mta.edu.vn

Nguyen. T. Tuan, Yoshihide Yamada
Universiti Teknologi Malaysia
Kuala Lumpur, Malaysia
Email: nguyentuan.dt9@gmail.com
ndayamada@yahoo.co.jp

Naobumi Michishita
National Defense Academy
Yokosuka Japan
Email: naobumi@nda.ac.jp

***Abstract* – In implantable antenna applications for human health care, normal-mode helical antenna (NMHA) is considered to be one of promising candidates. Due to antennas put inside human body, electromagnetic simulations are needed to model human body and clarify electrical characteristics of antennas. Electromagnetic performances of NMHA can be conveniently calculated by using Method of Moment (MoM). However, accuracies of calculated results were not clear. In this paper, another simulation method of finite element method (FEM) is employed as a reference. Calculated results such as self-resonant structures, electromagnetic field distributions, input impedances and radiation pattern are compared between MoM and FEM. Through very good agreements between two simulation methods, calculation accuracies of MoM are ensured.**

***Keyword* — NMHA; Human Body; FEKO; MoM; FEM.**

I. INTRODUCTION

Recently, many trials of applying radio wave devices for human healthcare are making. The ingestible, wearable and implantable antenna are the three types of antenna that is included in the human healthcare. For implantable applications, requirement for antenna size and efficiencies are very severe. Previously, some kinds of antennas were proposed for wireless capsule endoscopy (WCE) such as spiral antenna [1], conformal chandelier meander line antenna [2], loop antenna [3] and conformal patch antenna [4]. But antenna performances are not clarified yet when using in human body environment. The human tissues have a very high relative permittivity and some amount of conductivity. Thus, radio wave radiations from antennas contained in a human tissue will be weakened too much. Antennas that have high efficiency in very small sizes are strongly requested. For this purpose, a normal-mode helical antenna (NMHA) will be considered as a promising candidate because of having electric and magnetic current sources for radiations. Moreover, NMHA achieves a self-resonant characteristic that make impedance matching circuit very simple [5]. Previously, design methods and antenna performances were clarified in the free space condition [6][7]. In order to apply NMHA for implantable in a human body, antenna design methods and performances should be clarified.

In this paper, antenna self-resonant structures and antenna performances of small NMHA are clarified through electromagnetic simulations by a method of moment (MoM) scheme of a commercial electromagnetic simulator FEKO 7.0 [8]. The MoM calculations have features of small calculation time and small computer memory size. However, calculation accuracies of human muscle are not so clear. Therefore, another simulation method of finite element method (FEM) is employed as a reference. Calculation frequency of 2.4 GHz is selected by taking into account the implantation application frequency. Calculated results such as self-resonant structures, electromagnetic field distributions, input impedances and radiation pattern are compared between MoM and FEM. Through very good agreements between two simulation methods, calculation accuracies of MoM are ensured.

II. SIMULATION METHODS

Simulation model is shown in Fig.1. Electric constants are set based on a practical human muscle at 2.4 GHz [9]. NMHA is put inside a dielectric material of $\varepsilon_r = 53$. The wavelength in material (λ_g) is related to a wavelength in free space (λ_0) as follows:

$$\lambda_g = \frac{\lambda_0}{\sqrt{\varepsilon_r \mu_r}} \tag{1}$$

Then, wavelength in material (λ_g) becomes 17.15 mm. The model size of a human tissue of 30 mm is considered sufficient large compared to λ_g. Simulation methods of MoM and FEM are summarized in Table. I. In MoM scheme, electromagnetic fields inside a material are converted to surface fields of the material by the surface equivalent principle (SEP). In the FEM scheme, spacial electromagnetic fields are calculated. Simulation parameters are summarized in Table. II. Mesh sizes of material are changed to investigate accuracy of calculation. In this material size, computational memory size and times are not different so match between MoM and FEM.

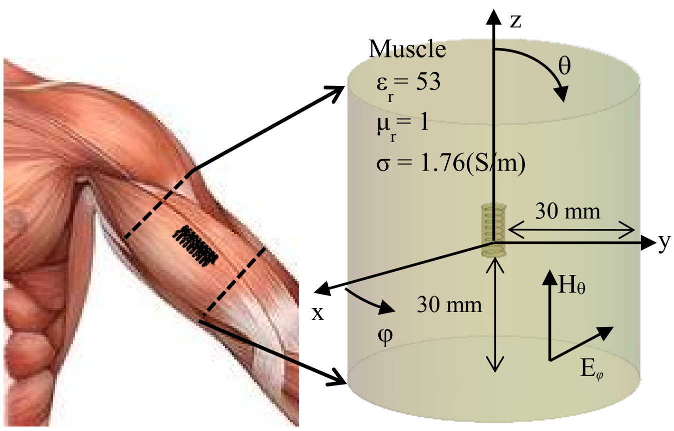

Fig. 1. Simulation model

TABLE I. SIMULATION METHODS of MoM and FEM

Scheme	Calculation method	Computer resources
MoM	• Calculate surface currents (2D distribution) • Surface is divided into small meshes	• Rather small memory
FEM	• Calculate spacial electromagnetic fields (3D distribution) • Space is divided into small volumes • Absorbing boundary is needed	• Large computer memory

TABLE II. SIMULATION PARAMETERS

Method	MoM	FEM
Frequency	2.4 GHz	2.4 GHz
Dielectric Constant	ε_r= 53; μ_r=1 σ = 1.76 (S/m)	ε_r= 53; μ_r=1 σ = 1.76 (S/m)
Mesh size of Antenna Wire	$\lambda_g/20$	$\lambda_g/20$
Mesh size of Material	$\lambda_g/3$; $\lambda_g/5$; $\lambda_g/7$	$\lambda_g/3$; $\lambda_g/5$; $\lambda_g/7$
Number of turns	N = 5; 7; 10	N = 5; 7; 10
Metallic wire	Copper (σ= 58 x 10^6 [1/Ωm])	Copper (σ= 58 x 10^6 [1/Ωm])
Memory	669 MB	1552 MB
Calculation time	0.46 h/sim	0.24 h/sim

III. SIMULATION RESULT

A. Convergence of results

In calculation, the structure of point A in Fig. 5 is used. In order to ensure calculation accuracy, different mesh sizes of a material such as $\lambda_g/3$; $\lambda_g/5$ and $\lambda_g/7$ are used. Calculation results of antenna input impedances by MoM and FEM are shown in Fig. 2 and Fig. 3, respectively. At mesh size of $\lambda_g/3$, 2.4 GHz point shifted from the resonant. However, at mesh size of $\lambda_g/5$ and $\lambda_g/7$, 2.4 GHz points become the resonant. Moreover, input impedance results agree very well in MoM and FEM calculations. Next, current distributions at 2.4 GHz are shown in Fig. 4. At mesh size of $\lambda_g/3$, current distribution becomes asymmetrical. At mesh sizes of $\lambda_g/5$ and $\lambda_g/7$, correct current distributions are obtained. As a result, mesh size of $\lambda_g/5$ and $\lambda_g/7$ are proper for correct calculation. In the following calculation, the mesh size of $\lambda_g/5$ will be utilized.

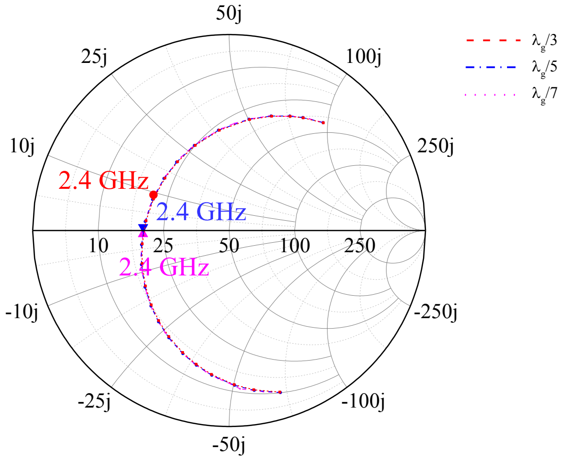

Fig. 2. Input impedance by MoM

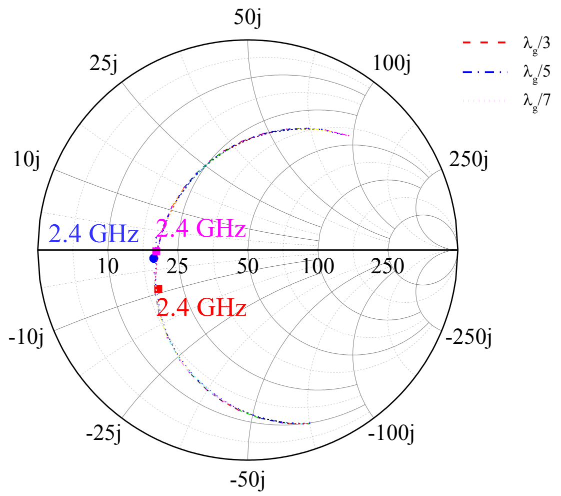

Fig. 3. Input impedance by FEM

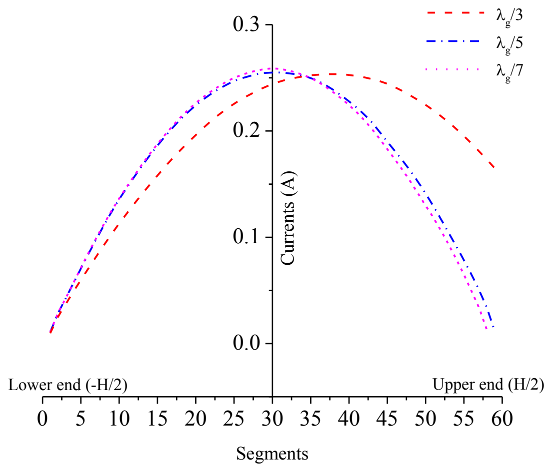

Fig. 4. Current distributions

B. Self-resonant structures

At the A point of Fig.5, resonances at 2.4 GHz are obtained as shown in Fig.2 and Fig.3. By checking resonances in input impedance charts for given structures, data for self-resonant structures are obtained. Results of self-resonant structures are shown in Fig. 5. Here, H and D indicate height, and diameter of an antenna, respectively. N indicates number of turn. Result of Fig.5 is similar to previous structures at 402MHz [10]. Resonant structures agree very well between MoM and FEM. Input impedance results at structures A and B are shown in Fig. 6. MoM and FEM results agree very well. As an important antenna parameter, VSWR are shown in Fig. 7. The bandwidth of A and B at VSWR = 2 are 63 MHz and 184 MHz, respectively. These correspond to fractional bandwidth of about 2.6% for A and 7.7% for B. Although bandwidths of NMHA are very narrow in a free space, bandwidths are increased in the human body condition. Because human body is considered as a wave absorber, antenna bandwidth is expanded by covered with an absorber.

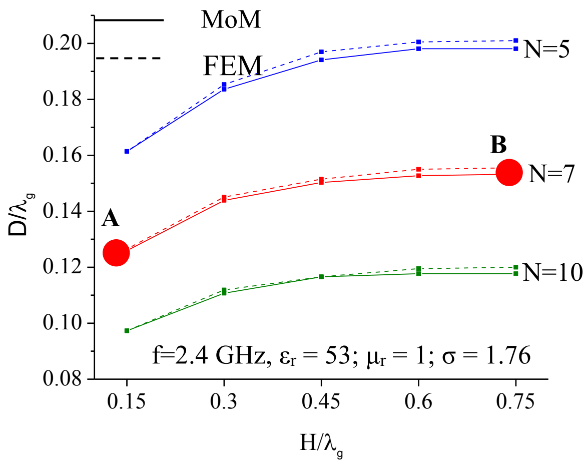

Fig. 5. Self - resonant structures

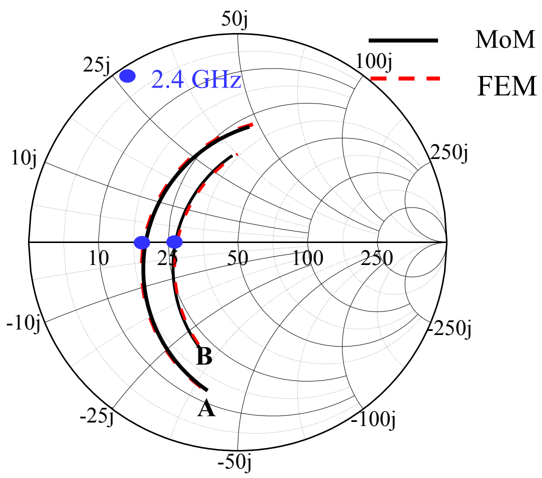

Fig. 6. Input impedaces at point A and B

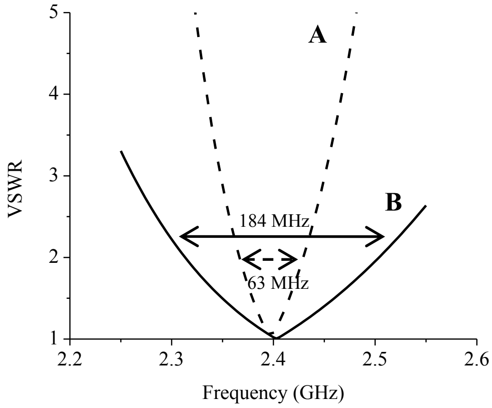

Fig. 7. Antenna bandwidth

C. Field distributions

In order to understand electromagnetic performances, near field distributions of structure A in Fig. 5 are obtained. Fig. 8 and Fig. 9 indicate magnetic field distributions and electric field distributions, respectively. Here NMHA is covered by a human muscle with relative permittivity ε_r= 53 and conductivity σ = 1.76 (S/m). Ares of human muscle is expressed by broken lines. Calculated results of MoM and FEM show good agreements. As a remarkable characteristic, electric and magnetic waves degrade rapidly inside a muscle. It is shown obviously that a muscle is considered as a wave absorber. When comparing magnetic and electric field distributions, fading of field in the muscle seems smaller in magnetic field.

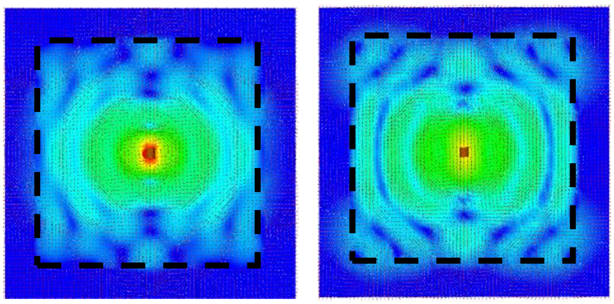

a) MoM b) FEM

Fig. 8. Magnetic field distributions (H_φ)

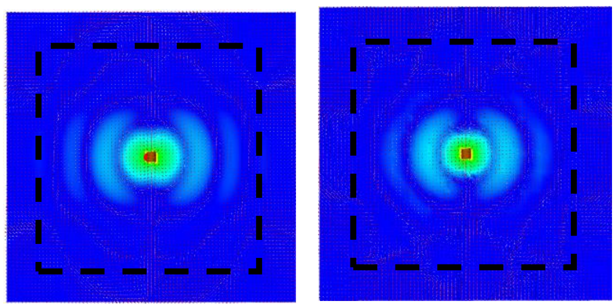

a) MoM b) FEM

Fig. 9. Electric field distributions (E_φ)

D. Input Resistance

Based on self-resonant curves in Fig. 5, input resistances are calculated. Comparisons of MoM and FEM results are shown in Fig.10. Input resistances become rather large. Because antenna is covered by a wave absorber, absorber resistance is included in the input resistance. The reason of large resistance is owing to large absorber resistance. One more interesting thing is resistance is increased depending on antenna volume increase.

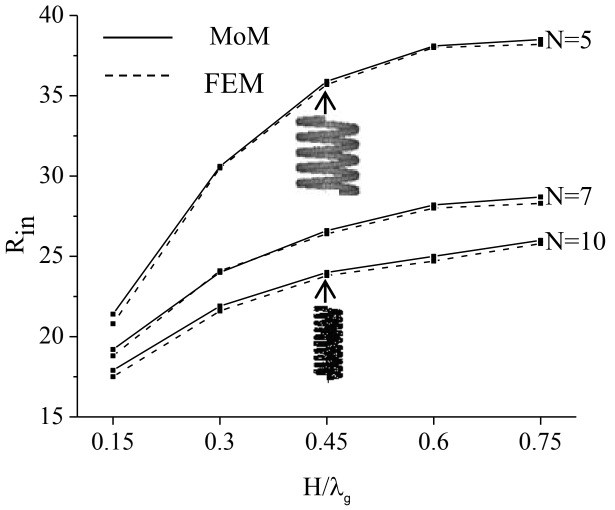

Fig. 10. Input Resistance

E. Radiation Pattern

Radiation characteristics of structure A in Fig. 5 are shown in Fig. 11 and Fig. 12. Radiation pattern becomes omnidirectional because of structural symmetry. Because of small antenna efficiency and surrounded by lossy dielectric, antenna gain become around -20 dBi and -30 dBi for $E_{\varphi Max}$ and $E_{\theta Max}$, respectively. Results of MoM and FEM have a good agreement.

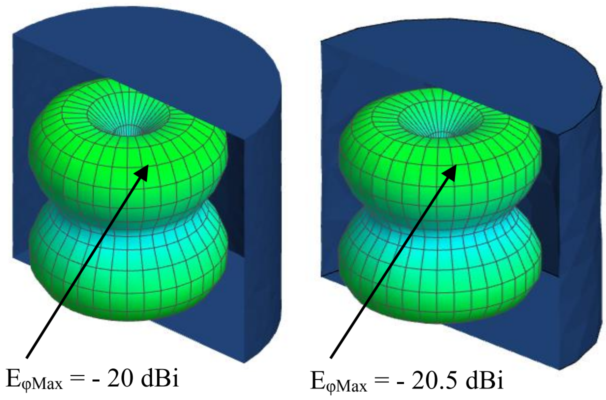

Fig. 11. Radiation pattern of NMHA (E_φ)

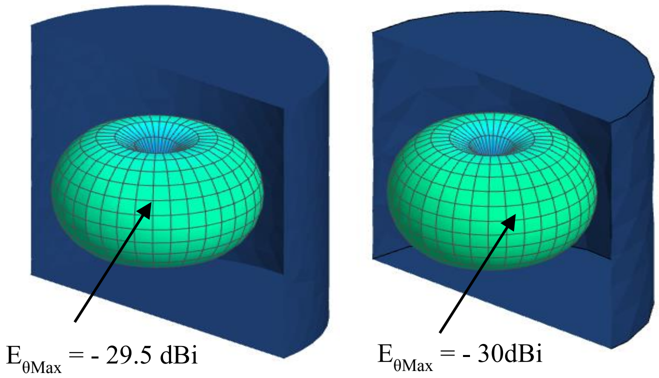

Fig. 12. Radiation pattern of NMHA (E_θ)

IV. CONCLUSION

Comparisons of calculation results by MoM and FEM for NMHA used in human body condition are made. Results for self-resonant structures, electromagnetic field distributions, input impedances and radiation patterns agree very well in two calculation methods. Calculation accuracies of MoM can be ensured. Moreover, NMHA performances in a human body conditions can be clarified.

REFERENCES

[1] S.I. Kwak, K. Chang and Y.J. Yoon, "Small spiral antenna for wideband capsule endoscope system," Electronics Letters, Vol. 42, Issue 23, pp. 1328 – 1329. November 2006.

[2] P. Izdebski, H. RAjagopalan and Y. Rahmat-Samii, "Conformal ingestible capsule antenna: A novel Chandelier meandered Design", Special issue IEEE Trans. Antennas and Propag, Feb 209. pp.900 - 909.

[3] S. Yun, K. Kim and S. Nam, "Outer wall loop antenna for ultra wideband capsule endoscope system", IEEE Antennas Wireless Propag. Lett. Vol. 9, pp. 1135 – 1138, Dec. 2010.

[4] E. G. Lim, Z. Wang, F. Z. Yu, T. Tillo and K. L. Man, "Transmitter Antennas for Wireless Capsule Endoscopy", SoC Design Conference (ISOCC), 2012 International. Pp. 269 – 272.

[5] Yoshihide Yamada and Naobumi Michishita, "Design Methods and Electrical Performances of Small Normal-Mode Helical Antennas," IEICE, Trans. Commun. B, vol. J96-B, no.9, pp.894-906, Sept. 2013.

[6] W.G.Hong, W.H.Jung, Y.Yamada and N.Michishita, "High performance Normal Mode Helical Antenna for RFID Tags", IEEE International Sympo. on Aut. and Prop., pp.6023-6026, June 2007.

[7] Quoc Dinh Nguyen, Naobumi Michishita, Yoshihide Yamada and Koji Nakatani, "Deterministic Equation for Self-Resonant Structures of Very Small Normal-Mode Helical Antennas", IEICE Trans.Commun., Vol.E94-B, No.5, PP.1276-1279, May 2011

[8] FEKO suite 7, EM Software & Systems

[9] Dmitriy D Karnaushenko, Daniil Karnaushenko, Denys Makarov and Oliver G Schmidt, "Compact helical antenna for smart implant applications ", NPG Asia Materials (2015) 7, e188; doi:10.1038/am.2015.53

[10] Nguyen Thanh Tuan, Yoshihide Yamada, Nguyen Quoc Dinh, Naobumi Michishita, "Self-Resonant Structures of Normal-Mode Helical Antennas embedded in Dielectric and Magnetic Materials", ATC, 627-632, ISSN 2162-1020, Oct 2015.